

RESEARCH ARTICLE

WILEY

Adaptive differential protection for transformers in grid-connected wind farms

Sujo Palamoottil George  | Sankar Ashok National Institute of Technology Calicut,
673601, India**Correspondence**Sujo Palamoottil George, National
Institute of Technology Calicut, 673601,
India.

Email: sujop709@gmail.com

Summary

In response to energy requirements and environmental concerns, renewable energy technologies including wind power are considered to be the potential alternatives. Generally, wind farms are integrated into the grid through a transformer, and its rating depends upon the capacity of wind farms. The fault current of the system to which wind farm is connected changes according to the wind generators in service as well as with the wind speed. The study shows that the existing differential relay for transformer protection mal-operates during fault interval according to the operating conditions of the wind farm. Under such conditions, the generalized characteristics for the differential relay of the transformer need modification. The protection scheme should be capable of functioning satisfactorily under various dynamic conditions of the wind, which can be achieved through adaptive relaying. In this work, an algorithm for transformer differential protection according to the variation in wind power injection is proposed. A case study of a typical wind farm shows that the proposed algorithm adaptively modifies the settings of the differential relay with varying wind farm currents, according to the wind generators in service, as well as with regard to different wind speed conditions. The modified algorithm is also validated using the experimental setup in the laboratory.

KEYWORDS

external faults, fault currents, power system protection, relays, transformers, wind farms

1 | INTRODUCTION

Distributed generation (DG) is one of the solutions for the sustaining energy shortage. The generation of electric power from renewable sources will be a major share of DG in the coming decades.^{1,2} Among the various renewable sources, the percentage of wind-based power is steadily increasing worldwide, including in India.³ Although wind farms can be operated in islanded as well as in grid-connected modes, they are usually connected to the grid because the wind generation alone cannot cover the power demand.⁴

The generation of electric power from a wind farm is normally at 400 or 690 V, which is usually stepped up to a higher level and connected to the grid through the transformers. The primary protection scheme adopted for transformers is differential protection which is to detect internal faults with a high degree of sensitivity, while also being simultaneously immune to the external faults, ie, through faults. Differential protection should also not to operate under conditions such as inrush, over excitation, and heavy current transformer (CT) saturation.⁵ There are many methods reported for the identification of internal faults from the operating conditions of the system. Methods such

as the differential current gradient,⁶ empirical Fourier transforms,⁷ parks vectors,⁸ geometrical structural analysis of waveform,⁹ wavelet transform^{10,11} probability concept¹² and decision tree-based discrimination,¹³ moving windows,¹⁴ and voltage and current ratios¹⁵ are proposed to discriminate internal faults from external faults, inrush, and over excitation conditions. Harmonic restraint methods are commonly used in industries for the detection of inrush and over excitation conditions of the transformers. The second harmonic component in the inrush current is used to detect whether the transformer is experiencing inrush or faulty conditions, and the fifth harmonic component is used to identify the fault conditions.¹⁶ A modified harmonic restraint-based relay is proposed in Zheng et al¹⁷ to avoid the mal-operation of the relay during the nonsynchronous energization of the transformer. Single slope and dual slope characteristics suggested in a technical manual¹⁸ provide sensitivity towards internal fault as well as security to the external fault. This can be achieved by adjusting the slope characteristics. The existing algorithms for single slope and dual slope differential relay make use of harmonic restraint method for avoiding unnecessary tripping during inrush and over excitation conditions.¹⁹ The dual slope characteristics with 2 breaking points and a smooth curve between them are suggested in Sevov et al²⁰ to avoid relay mal-function during external fault condition by the early detection of the CT saturation. The symmetrical component of the current is used to detect and issue the trip signal for the minute internal fault at the incipient stage.²¹

There are problems associated with the integration of wind energy into the grid, especially with the protection system, due to the intermittent nature of wind.^{22,23} The dynamic nature of the wind profile may result in the mal-operation of transformer differential relays during fault intervals. This has been reported by many substations connecting wind farms to the grid.²⁴ The settings of the relay need to be changed faster for the reliable operation and to build a system that works for a broad range of operating conditions without introducing much time delay. This is where an adaptive protection algorithm comes into play. Adaptive protection permits and seeks to make adjustments to protection functions in order to make them more attuned to prevailing power system conditions, which include planned and unplanned switching operations, and the addition of distributed energy resources. The coordination of over current relays based on adaptive relaying techniques is proposed in Ojaghi et al.²⁵ The settings of over current relays are modified according to grid-connected as well as with islanded mode of operation and also with different loading conditions. An adaptive differential protection for the 3-phase transformer is proposed in Oliveira et al²⁶ in which the restriction zone is increased or decreased according to different operating conditions. An adaptive multiregional differential relay is given in Dashti and Sanaye-Pasand,²⁷ in which dual slope differential characteristics are divided into 5 operating regions to provide correct decisions for mild, heavy, severe internal faults, external faults with CT saturation, and inrush conditions. The fault component of the restraint and differential currents is used to adaptively adjust the settings of the dual-slope characteristics according to the disturbances and discriminates external and internal faults.²⁸

However, the algorithms addressed for the adaptive relays for transformer differential protection do not consider the dynamic conditions of the wind farms during fault period. The differential relay characteristics must be adapted to the presence of wind farms due to its intermittent nature. The settings of the differential relay need to be altered according to the variation in fault level due to the changes in wind power output as well as with the number of wind generators in service. An algorithm for the differential relay that can self-modify its tripping characteristics according to wind power output is proposed, and it is validated with the experimental results. A case study conducted for a typical wind farm shows that the proposed method avoids mal-operation of the differential relay in varying wind power conditions.

2 | PROPOSED ALGORITHM FOR ADAPTIVE DIFFERENTIAL RELAY

The tripping criteria for the single slope transformer differential relay can be expressed as

$$I_d \geq I_{pickup} \quad (1)$$

$$I_d \geq KI_r \text{ where } I_d = I_1 - I_2 \text{ and } I_r = \frac{I_1 + I_2}{2} \quad (2)$$

$$\text{Combining (1) and (2) } I_d \geq I_{pickup} + KI_r \quad (3)$$

Here, I_d is the fundamental component of differential current, I_r is the restraining current, I_{pickup} is the pickup value of current, I_1 , I_2 are primary and secondary currents, and K is the slope of the differential relay. The pickup current

setting should be greater than the magnetizing current of the CT. Equation 3 represents single slope characteristics of the differential relay. If the operating point lies above the slope, the differential relay trips and the relay restrains if the operating point is below the slope. The steeper the slope is, the relay will be more immune to the external faults but will be less sensitive to the internal faults involving high resistance. Hence, the slope is set at a compromised value so that relay is more sensitive to internal faults and more selective to external faults. Figure 1 shows the single slope characteristics of transformer differential protection (shown as the dotted line, PQR). The operating point A $[(I_{1intmin} + I_{2intmin}) / 2, (I_{1intmin} - I_{2intmin})]$ corresponds to the minimum internal fault, where $I_{1intmin}$ and $I_{2intmin}$ are minimum internal fault current at primary and secondary side, respectively. The minimum internal fault occurs during the turn to turn fault which involves only 2 turns. The slope K is fixed in such a way that the minimum internal fault operating point must be in tripping region, and the pickup current is slightly below this point. The slope K is selected to provide sensitivity towards the minimum internal fault as the operating point is denoted by "A."

The differential protection with single slope characteristics does not provide stability during severe external fault conditions. The maximum external fault is given by the operating point B, $[(I_{1extmax} + I_{2extmax}) / 2, (I_{1extmax} - I_{2extmax})]$, where $I_{1extmax}$ and $I_{2extmax}$ are primary and secondary current during maximum external fault condition, respectively. The maximum external fault occurs during 3-phase short circuit fault involving low resistance. If the operating point B is in tripping region and during these circumstances, there are chances of relay mal-function and it must be avoided. A dual slope characteristic (shown as the bold line, PQS in the Figure 1) with 2 slopes K and K_m is necessary such that the relay mal-operations can be prevented. The second slope K_m with higher value provides necessary security towards the external faults. The slope K_m is fixed based on the rated operating conditions of the system.

The tripping criterion for dual slope relay is formulated as:

$$\text{Case 1: } |I_r| \leq |I_{rt}|. \quad (4)$$

If $I_d \geq K|I_r| + I_{pickup}$, then trip the differential relay.

$$\text{Case 2: } |I_r| \geq |I_{rt}| \quad (5)$$

If $I_d \geq K_m |I_r| - (K_m - K)I_{rt} + I_{pickup}$, then trip the differential relay.

The dual slope percentage biased restraining characteristics can be determined by the following settings: (1) I_{pickup} is the pickup current setting, (2) K is the lower percentage bias setting, (3) I_{rt} is the bias current threshold setting or the crossover point, and (4) K_m is the higher percentage bias setting.

In differential relays for the substation transformers with wind farm integration, dual slope characteristics are to be modified for avoiding mal-operation during external fault conditions. This is due to the variation of short circuit current from wind farm, which depends upon the varying wind power.

The short circuit current from the wind farm is

$$I_{SC} = \sum_{k=1}^N k I_w \quad (6)$$

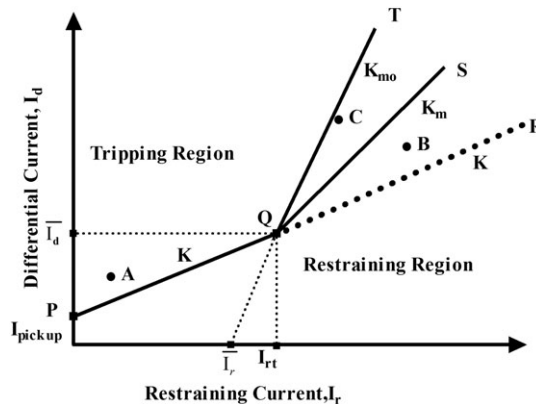


FIGURE 1 Relay characteristics of single slope, dual slope, and modified dual slope differential protection

where I_{SC} is the total short circuit current from the wind farm, I_w is the fault current from a single wind generator, N is the total number of wind generators in wind farm, and k is the number of wind generator in service. The current I_w , from the wind generator, depends upon the source impedance of each generator.

$$I_w = \frac{E''}{X''} \quad (7)$$

where E'' is the sub transient internal voltage of the generator at the moment of short-circuit and X'' is the sub-transient reactance of the generator which is neglected due to low value of armature resistance. The internal voltage can be expressed as

$$E'' = V_t + I_l X'' \quad (8)$$

$$I_w = \frac{V_t + I_l X''}{X''} \quad (9)$$

where V_t and I_l are the terminal voltage and the current of the wind generator, respectively. The current contribution of a fixed-speed wind turbine is directly proportional to the wind speed. Maximum current is supplied at the rated wind speed and rated power output. For all other wind speeds, the current decreases, and hence the short circuit contribution reduces.

When the wind speed is below the cut-in speed, the power output of the wind generator is zero. The brakes are applied when the speed reaches the cut-out speed, and the machine stops generation. The fault contribution from each wind generator is varying according to wind speed which is between the cut-in and cut-out speed of the wind turbine. Accordingly, the short circuit current contribution from the wind farm is varying which results in dynamic shifting of operating points. The operating point C represents the external fault operating point when the wind farm is working below its rated condition. The operating point C, given by $[(I_{1extmin} + I_{2extmin}) / 2, (I_{1extmin} - I_{2extmin})]$ where $I_{1extmin}$ and $I_{2extmin}$ are primary and secondary current during external fault condition, respectively. The fault current from wind farm varies according to the number of wind generators in service as well as with the wind power output. The dual slope characteristic for the differential relay for transformers with wind farm integration mal-operates during external fault conditions as the point "C" is in tripping zone. The operating point during external fault condition comes in the tripping zone and the differential relay issues unnecessary trip signal. Therefore, the differential relay settings of the transformer have to be altered according to the fault level which varies with power output from the wind farm. This can be achieved by modified dual slope characteristics, which is represented as PQT in Figure 1.

The modified dual slope characteristics of differential relay can be written as 2 straight line equations shown in Figure 1. In the modified dual slope characteristics, I_{pickup} , K , and I_{rt} are same as those of single slope characteristics. The first straight line is given by Equation 3. Beyond the crossover point I_{rt} , the straight line QS can be formulated as

$$I_d = K_m (I_r - \bar{I}_r) \quad \text{and} \quad K_m = \frac{\bar{I}_d}{I_{rt} - \bar{I}_r} \quad (10)$$

\bar{I}_r is the restraining current at $I_1 = I_2$ ($I_d = 0$) \bar{I}_r and \bar{I}_d is the differential current corresponding to I_{rt} . In Equation 10, the second slope K_m is changing according to the operating conditions of the wind farm. The maximum fault current contribution is during when all the wind generators in wind farm are in service and minimum fault level is during when no wind generators are in service. The modified characteristics for the transformer differential relay can be written as

$$I_d \geq \bar{K}_m |I_r| (\bar{K}_m - K) I_{rt} + I_{pickup} \quad (11)$$

where \bar{K}_m is the variable slope which is changing according to the fault level contribution from the wind farm.

Figure 2 shows the trajectory of operating point during internal and external fault conditions. The turn-to-turn internal fault is varied from 2 turns shorted (I_{intmin}) to the short circuit in 80% winding (I_{intmax}). The pickup current (I_{pickup}), initial slope (K), and crossover point to the second slope (I_{rt}) should be selected in such a way that the operating points during internal fault conditions must be in the tripping region. The internal fault operating points will not vary with the

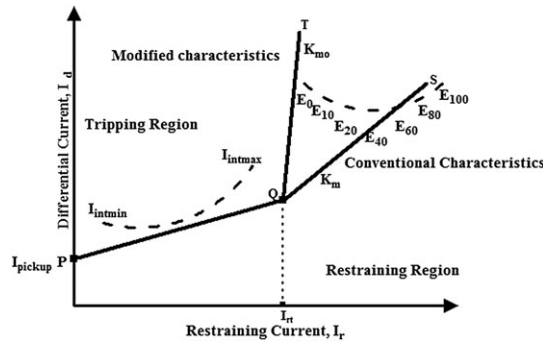


FIGURE 2 Trajectory of operating points during internal and external faults

load conditions and also with the wind power output from the wind farm. However, the external fault operating points are varying with the wind power penetration. The conventional relay settings are fixed based on the rated operating conditions of the wind farm. E_{100} represents the external fault operating point, when all the wind generators in the wind farm are in service. The external fault operating point is shifted to E_0 , when none of the wind generators are in service. Therefore, the characteristics of the dual slope relay need to be shifted from PQS to PQT to maintain the security towards the external fault conditions. The second slope needs to be modified adaptively from K_m to K_{mo} , according to the operating conditions of the wind farm.

The algorithm for the proposed adaptive relaying technique of the transformer differential protection is shown in Figure 3. The reading from primary and secondary CTs of the power transformer and current from the wind farm are measured. The tripping signal during inrush and over excitation conditions are blocked by harmonic restraint method. Based on the total installed capacity of the wind farm, the setting points of the pickup current, initial and final slopes, and change over points of the slopes are fixed. The tripping signal is issued when the differential current exceeds the percentage of the restraining current (Equations 3 and 11). The algorithm updates the set points of the differential relay according to the measured value of wind farm current. The algorithm continuously monitors the wind farm current, and the setting is dynamically modified according to the wind generators in service as well as with the wind speed. The total wind farm current, I_{WF} , is fed to the current sensors of the numerical differential relay in which the algorithm is written, and the settings are updated.

3 | EXPERIMENTAL VERIFICATION OF THE PROPOSED ALGORITHM FOR THE TRANSFORMER DIFFERENTIAL PROTECTION

The block diagram of the experimental setup is given in Figure 4. The proposed algorithm is tested using the transformer protection unit (Figure 5) with the programmable numerical differential relay by ASHIDA-ADR 133A.²⁹ The unit consist of a 3 kVA, 415/415V, Y-Y connected transformer. The various internal and external faults are injected, and the trip status of the relay is noted. The details of the unit are given in the Appendix (Table A1). In the experimentation, the wind farm supply is replaced by a voltage source which is connected to the secondary side of the transformer through the synchronizing switch. The simulation and the experimentation are carried out with (1) 1 voltage source and (2) 2 voltage sources in the secondary side of the transformer, respectively.

Figure 6 shows the primary current, secondary current, and the trip signal for the transformer differential protection simulated in 3 kVA 415/415 V 3-phase transformer. The dual slope relay settings for the differential relay, with 2 voltage sources connected to the system, are shown in Table 1. The internal fault taken into consideration is turn-to-turn fault (2 turns) which is less sensitive as the differential current is small. The differential relay issues trip signal for internal fault at 5 seconds (Figure 6A). The external fault considered is LLL fault which is inserted at 5 seconds in the secondary side of the transformer. The dual slope setting is appropriate, as the relay does not mal-operate with regard to the external fault conditions (Figure 6B). The simulated case is validated with the experimental result which is shown in Figure 7.

The existing dual slope algorithm for the transformer differential protection is not suitable when there is a variation in number of voltage sources at the secondary side. The fault current will change according to the number of the voltage sources. The operating point during external fault conditions with a single source and 2 voltage sources in the secondary

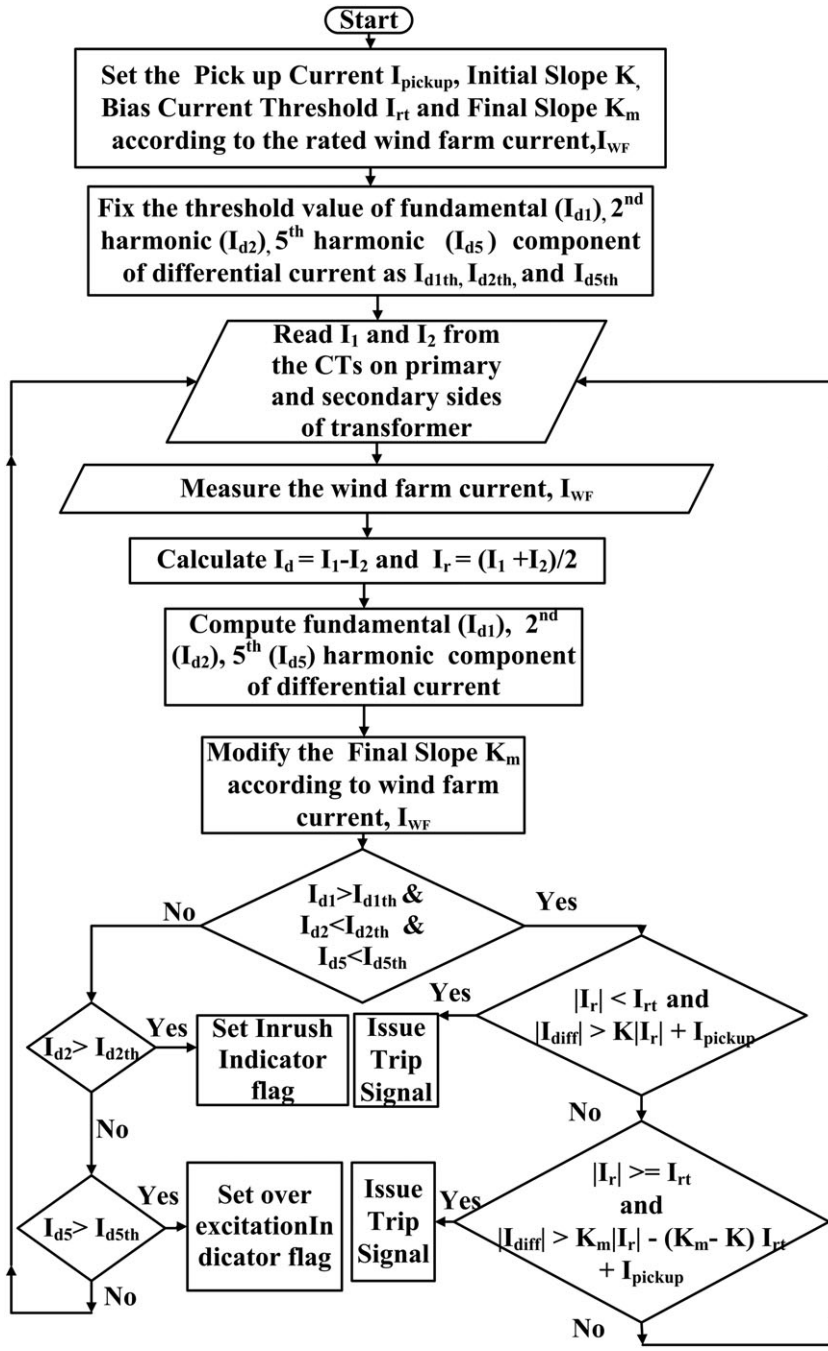


FIGURE 3 Algorithm for adaptive relaying for transformer differential protection

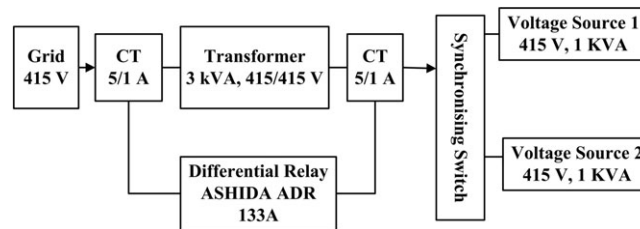


FIGURE 4 Block diagram for the experimental setup in the laboratory

side is shown in Figure 8. PQS is the characteristics selected with a slope of 70%, for the condition in which 2 voltage sources are connected to the secondary side. E_{1v} and E_{2v} are the external fault operating points with single and 2 voltage sources at the secondary side. The operating point E_{1v} is in tripping zone which causes the mal-operation of the relay for

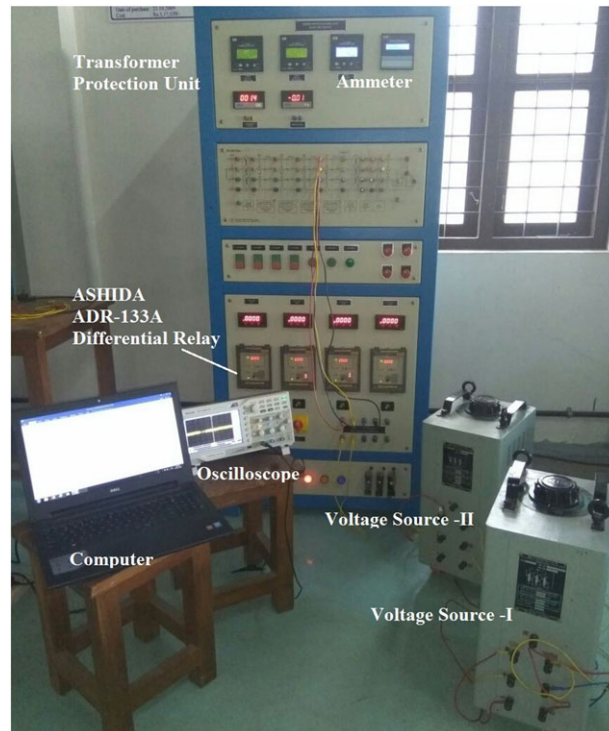


FIGURE 5 Transformer protection unit with the differential relay and voltage sources at the secondary side

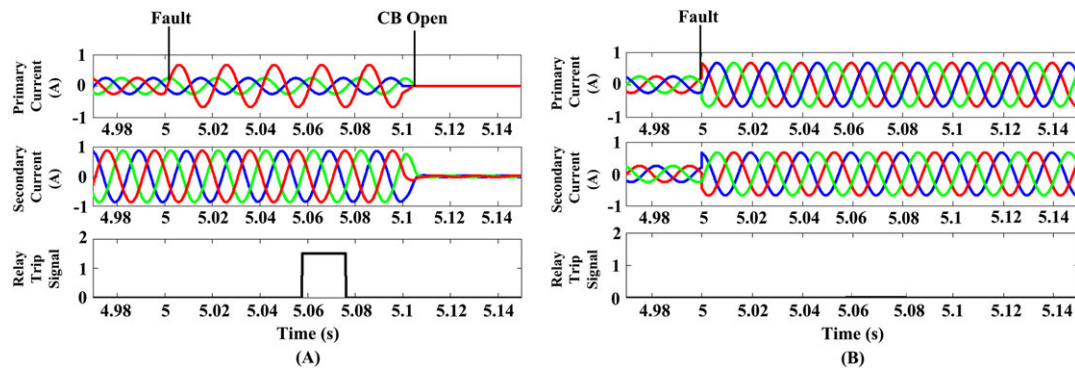


FIGURE 6 Primary current, secondary current, and trip signal for the dual slope differential relay with 2 voltage sources at the secondary side: A, internal fault; B, external fault

TABLE 1 Relay setting for dual slope differential relay (with 2 voltage sources at the secondary side)

Load Condition	Pickup Current, A	K_1 (Initial Slope)	Crossover Point (A)	K_m (Final Slope)
Two voltage sources at the secondary side	0.11	20	0.50	70

the characteristics PQS during external fault conditions. Therefore, the characteristics need to be shifted from PQS to PQT, ie, from 70% to 80% of the K_m value.

The primary current, secondary current, and trip signal of the differential relay with a single voltage source at the secondary side are given in Figures 9 and 10. The differential relay mal-operates for external fault as operating point is in the tripping zone. The relay issues trip signal for low intensity inter turn fault which is taken into consideration, by the proposed algorithm.

The differential relay characteristics need to be modified with the new settings as shown in Table 2, in order to avoid mal-operation. The threshold value of the second slope value, K_m , has to be changed by the removal of voltage sources at the secondary side.

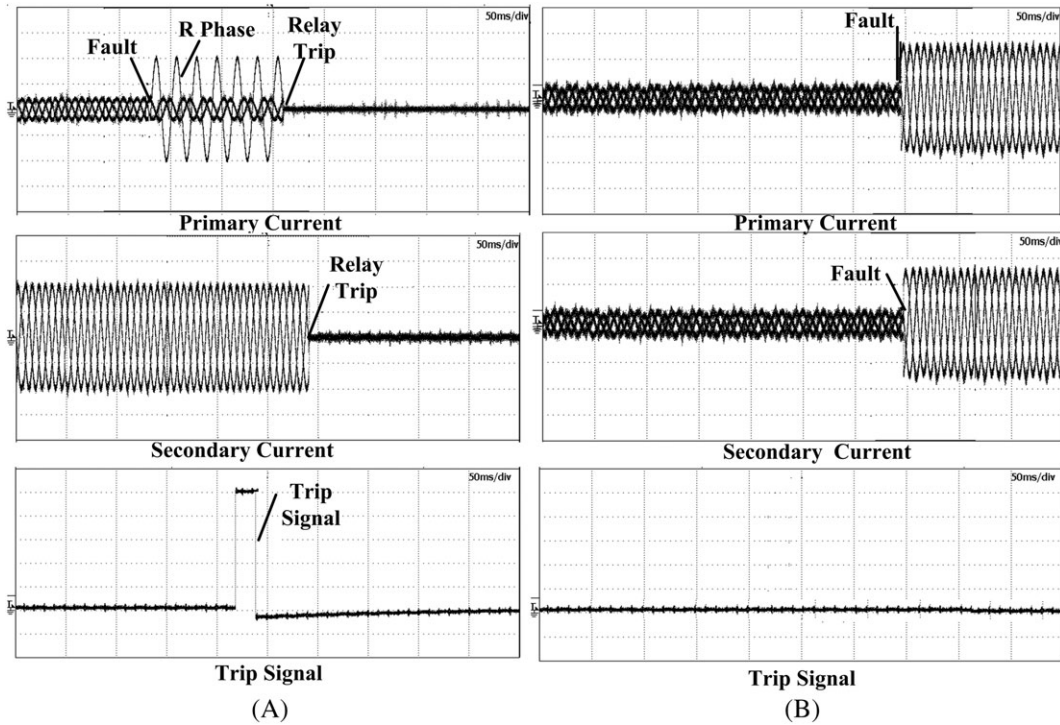


FIGURE 7 Experimental results for the primary current, secondary current, and trip signal with 2 voltage sources at the secondary side: A, internal fault; B, external fault [Y: 0.5 A/div, X: 50 ms /div]

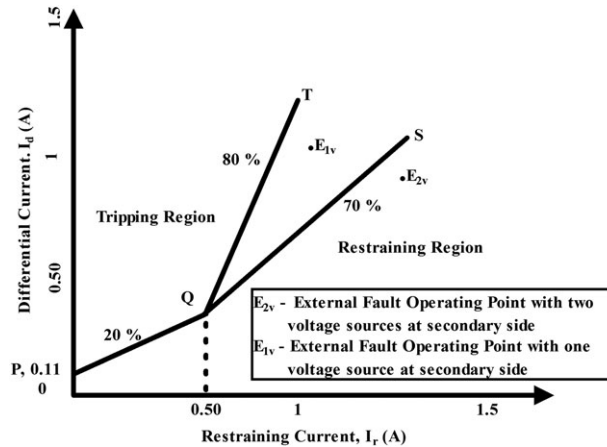


FIGURE 8 External fault operating point according to the variation in number of voltage sources at the secondary side

The comparison between the simulated and experimental results is given in Figure 11. The internal fault operating point from the simulation and experimentation is represented as I_{sim} and I_{exp} , respectively. The internal fault operating point remains same for the single and 2 voltage sources at the secondary side. The time of operation of the differential relay for the internal fault in the simulation is 38 and 50 ms in experimental results. The difference in the operating time is due to the CT measurement error. The external fault operating point is varying according to the number of voltage sources connected to the secondary side. The simulated and experimental results for the external fault operating points when 2 voltage sources at the secondary side are given as E_{2vsim} and E_{2vexp} , respectively. The points E_{2vsim} and E_{2vexp} are in the non tripping zone, and the relay does not issue the trip signal. It is observed that the external fault operating point is shifted to E_{1vsim} and E_{1vexp} in the simulated and experimental studies, when the number of voltage source at the secondary side is reduced to one. The points E_{1vsim} and E_{1vexp} is in the tripping zone and the relay mal-operates. In order to avoid the mal-operation the second slope, K_m is changed from 70% to 80%.

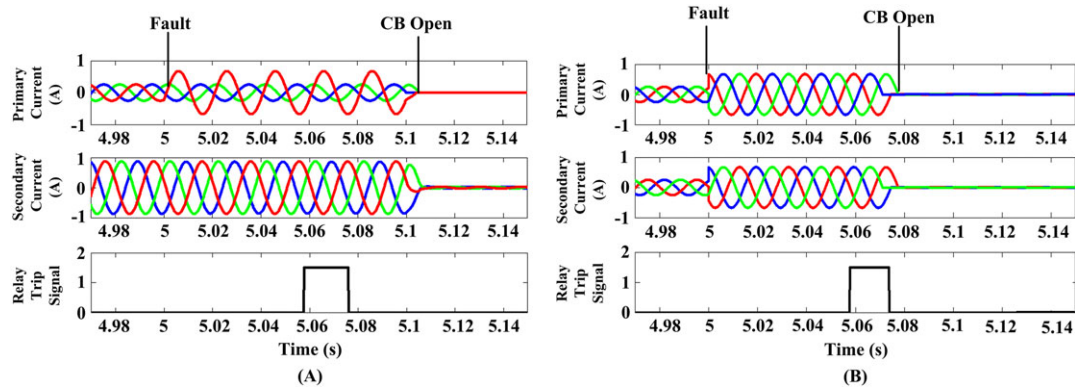


FIGURE 9 Primary current, secondary current, and trip signal for the dual slope differential relay with 1 voltage source at the secondary side: A, internal fault; B, external fault

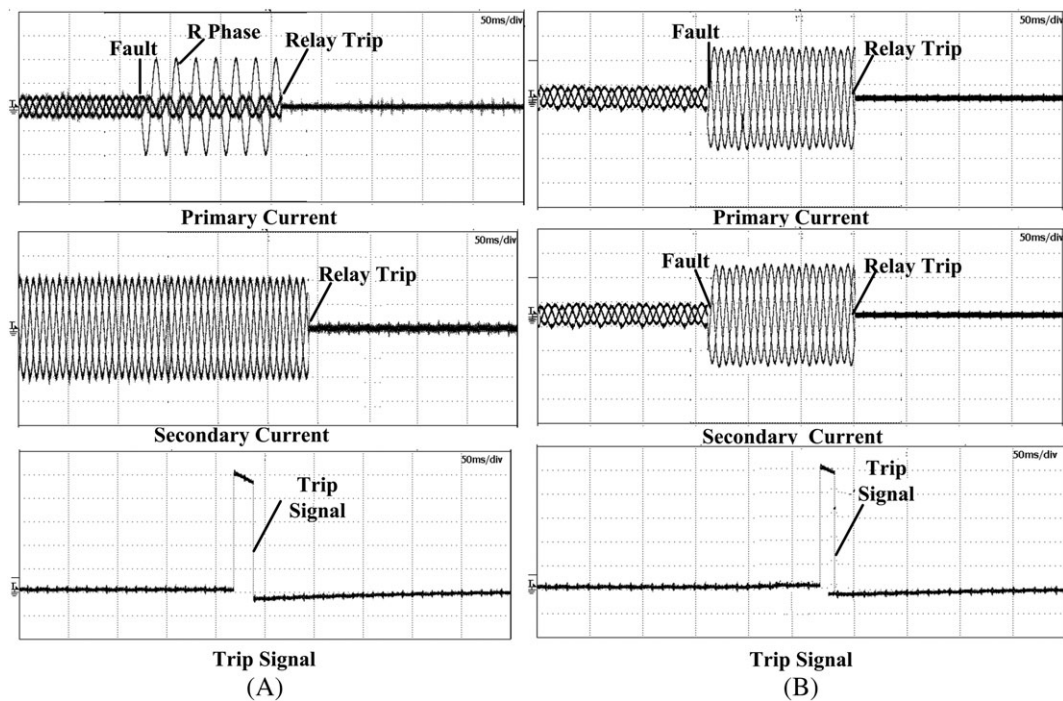


FIGURE 10 Experimental results for the primary current, secondary current, and trip signal with 1 voltage source at the secondary side: A, internal fault; B, external fault [Y: 0.5 A/div, X: 50 ms/div]

TABLE 2 Relay setting for dual slope differential relay (with 1 voltage source at the secondary side)

Load Condition	Pickup Current, A	K_1 (Initial Slope)	Crossover Point, A	K_m (Final Slope)
One voltage source at the secondary side	0.11	20	0.50	80

4 | CASE STUDY

The proposed algorithm for transformer differential protection is applicable to any systems where a wind farm is integrated into the grid via the substation transformer. The above adaptive relaying technique is applied to a transformer connecting a typical wind farm to the grid (Figure 12).³⁰ The different system conditions were analyzed by simulation. The wind farm has a total of 19 units of Vestas NM48 750 kW wind turbines with Squirrel Cage Induction Generator (SCIG) which has 2 sets of winding mechanisms of 6 poles and 8 poles each for 1000 and 750 rpm synchronous speed, respectively. The cut-in and cut-out speed for the 6-pole machine is 960 and 1040 rpm, and for the 8-pole machine, it is

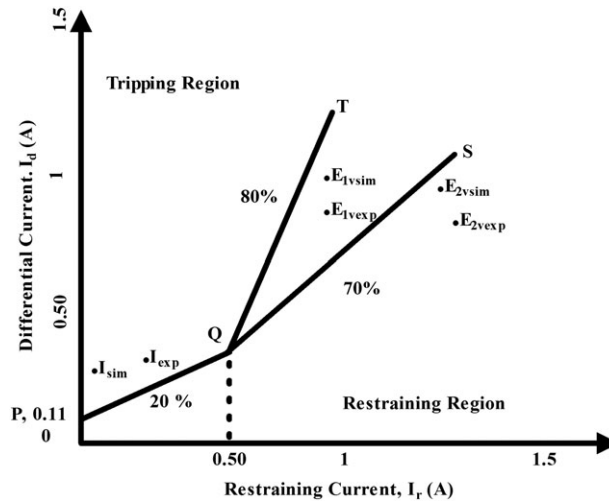


FIGURE 11 Comparison between simulated and experimental results for the modified dual slope transformer differential protection

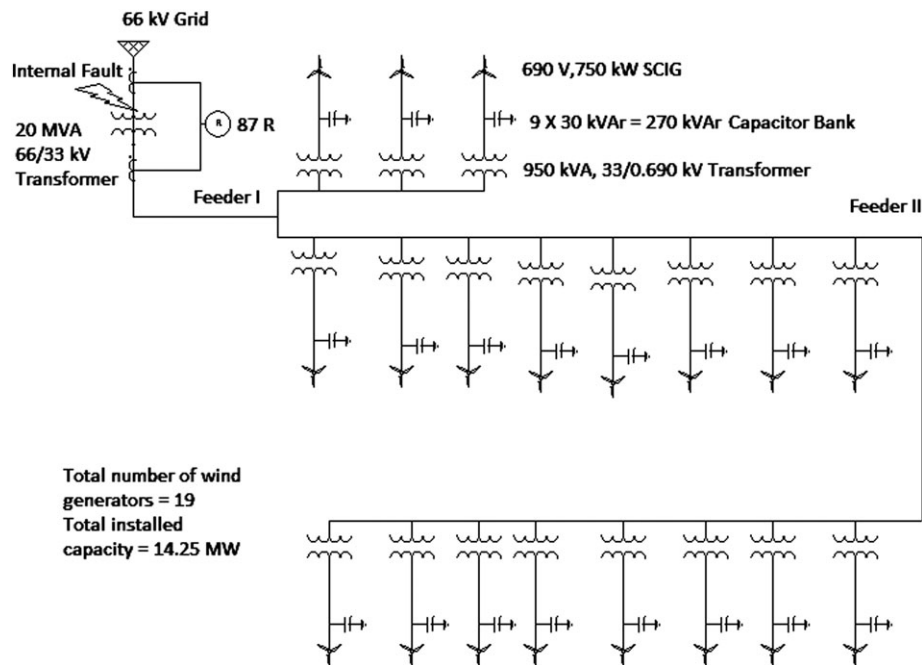


FIGURE 12 Wind farm layout of a typical wind farm

1480 and 1520 rpm, respectively. The SCIG output is at 690 V with a frequency of 50 Hz. The detail of the network is given in the Appendix (Table A2).

The wind generators are connected to 2 feeders, feeder I and feeder II. Three wind generators are connected to the feeder I, while 16 wind generators are connected to feeder II. The capacity of each wind generator is 0.75 MW with a total installed capacity of 14.25 MW. This is stepped up to 33 kV, by the transformer assigned to each wind generator. The rating of the transformer is 950 kVA, 0.690/33 kV. The 2 feeders are connected to a 20 MVA, 33/66 kV transformer before connecting to the grid. In the case study, there is no load connected to the wind farm side and hence $I_2 = I_{WF}$. The protection device used in the wind generator is a 63 A High Rupturing Capacity fuse. The transformer protection is achieved using a differential relay of make AREVA MiCOM P633 with the dual slope characteristics. As the wind farm is only connected to the grid, it does not have any isolated load; therefore, there is no possibility of employing the islanding mode of operation. The induction generator requires reactive power from the grid to avoid a voltage drop and a low power factor. The 9 capacitor banks, each of which is 30 kVAr, are used for reactive power compensation in this case.

The simulation is carried out for internal faults and external faults on the primary side and secondary side of the substation transformer using Power System Computer Aided Design (PSCAD) 4.2.0 software. The relay setting is normally fixed by assuming that all wind generators are present in the system and running at its rated capacity. The dual slope differential relay has 4 settings:

1) Pickup current setting—The pickup current setting should be greater than the magnetizing current. The setting can vary between 5% and 20% of the differential current. The pickup current setting is fixed as 0.13 A in the differential relay for the transformer in the case study.

2) Initial slope—The initial slope is set to allow for off-nominal tap settings and CT mismatch error. Normally, 1.25% is provided for each tap, and the slope can vary between 10% and 40%. Here, the slope is taken as 25%.

3) Crossover point to the second slope—The beginning of the second slope is greater than the rated current to cater for heavy through fault conditions. The break point can vary between 0.5 and 1.5 pu of current. The changeover point is taken as 0.57 A of the CT secondary current in this case.

4) Final slope—The value of the slope should be selected in such a way that it should provide selectivity towards external fault. The range of the slope can vary in between 40% and 70%. The slope value is selected such a way that it should provide security towards minimum external fault. The second slope value is fixed as 55% in this case. The above values are chosen in such a way that all the wind generators are working at its rated operating condition, and it is given in Table 3.

The minimum internal fault current happens during the turn-to-turn fault in the transformer winding, which involves 2 turns. The external fault occurs on the wind farm side which is external to the protection zone of the transformer under consideration and the minimum fault occurs during the line to ground fault. The simulation has been done for various internal and external faults including turn to ground fault, turn-to-turn fault, winding to core fault, LG, LLG, LLL, and LLLG faults. The short circuit current contribution from a single wind generator is small but from the wind farm makes it comparatively higher value. The value of fault current depends on the size of the wind farm. For a larger wind farm, the fault current is comparable with that of the grid. Hence, the relay setting needs to be modified for a better degree of protection.

The second harmonic component and the fifth harmonic component are used to identify the inrush as well as over excitation conditions in the transformer. The transformer is energized at 1 second, with a step increase in voltage is given at 2 seconds. The threshold value of the second harmonic and fifth harmonic components is fixed at 30%. Under inrush and over excitation conditions, the harmonic component exceeds the threshold value, and the proposed algorithm did not issue the trip signal for the differential relay by the harmonic restraint method. Table 4 gives the result.

The proposed algorithm discriminates internal faults from the external faults. In addition to the above, it takes care of mal-functioning of relay under inrush and over excitation conditions. The adaptive nature makes the algorithm for differential relay suitable for the dynamic conditions of the wind farm. Islanded operation is required in order to isolate the wind farm from the system when there is a fault either in the grid or on the wind farm side. This is achieved by over current relay provided in the primary side of the transformer. During internal fault conditions, the tripping criterion given by the (3) and (11) has to be satisfied, and the trip signal is issued.

Figure 13 shows the current waveforms (primary current and secondary current) and the trip signal during internal fault conditions, when all the 19 wind generators are in service. The dual slope relay settings for the differential relay

TABLE 3 Relay setting for dual slope differential relay (19 wind generators)

Wind Generators in Service	Pickup Current, A	K_1 (Initial Slope)	Crossover Point, A	K_m (Final Slope)
19	0.13	25	0.57	55

TABLE 4 Harmonic components of the differential current during the inrush and the over excitation condition of the transformer

Harmonic Components	Inrush Condition, %	Over Excitation Condition, %
Second	52.8	4.53
Third	27.23	9.67
Fourth	22.58	24.55
Fifth	18.57	46.77

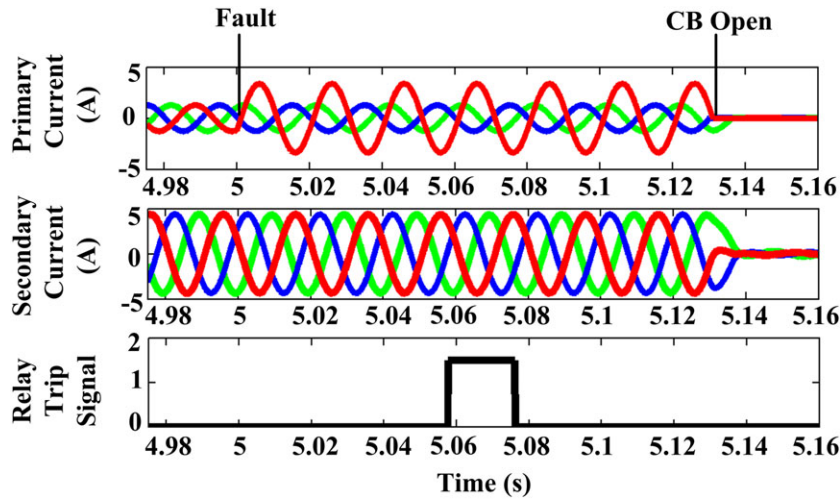


FIGURE 13 Primary current, secondary current, and trip signal for the dual slope differential relay during internal fault (all 19 wind generators are in service)

with all wind generators connected to the system are shown in Table 3. The internal fault taken into consideration is turn-to-turn fault (2 turns) which is less sensitive as the differential current is small. The differential relay issues trip signal for internal fault at 5 seconds. The external fault considered is LLL fault which is inserted at 5.2 seconds in the wind farm side. The setting is appropriate, as the relay does not mal-operate with regard to the external fault conditions. Figure 14 show that the differential relay does not issue tripping signals for the external fault. The simulated CT secondary values are compared with the measured values, and the error was found to be in the order of 0.02%. The differences in the values are due to the measurement error of the CTs.

The problem associated with wind power penetration is its intermittent nature based on the availability of wind. The existing relay setting is carried out by assuming that all wind generators are present in the system. Figure 15 shows the external fault operating point for 19 and 10 wind generators in services (E_{19} and E_{10} , respectively). PQS represents the characteristics selected for all the wind generators in service. When the number of wind generators in service is reduced, the external fault operating point is shifted from E_{19} to E_{10} as shown in Figure 15. The differential relay mal-operates as the operating point E_{10} is the tripping zone of the PQS characteristics.

The primary current, secondary current, and trip signal of the differential relay for the wind farms which is operating at its reduced capacity are given in Figures 16 and 17. The relay issues trip signal for low intensity inter turn fault which is taken into consideration, by the proposed algorithm (Figure 16). The wind generator in service is reduced to 10, and the relay mal-operates for external fault as operating point is in the tripping zone. Figure 17 shows the mal-operation of the differential relay when there is a reduced number of wind generators. The differential relay mal-functions as it trips for the secondary side (wind farm side) external fault which is inserted at 5.2 seconds.

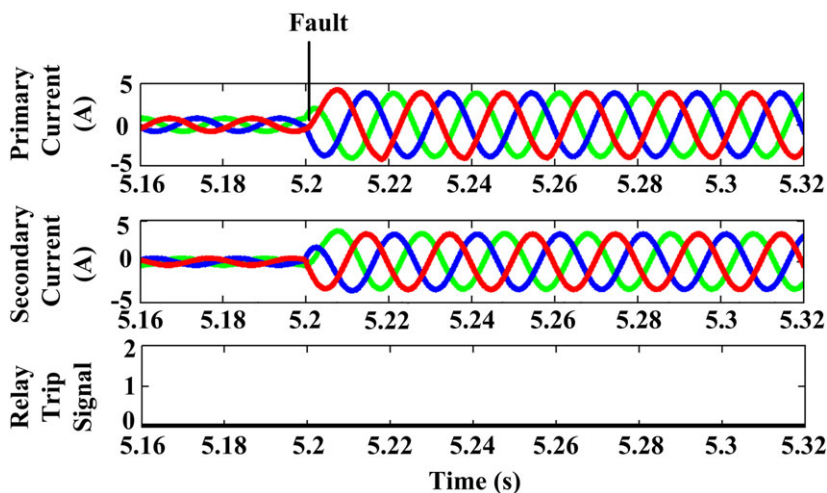


FIGURE 14 Primary current, secondary current, and trip signal for the dual slope differential relay during external fault (all 19 wind generators are in service)

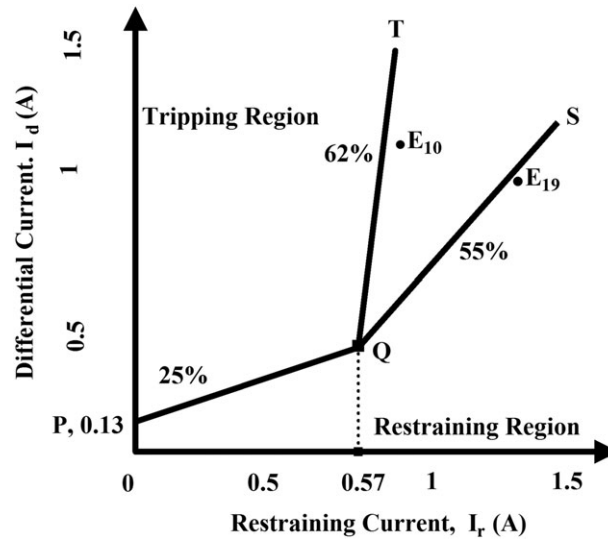


FIGURE 15 External fault operating point according to the variation in wind power penetration

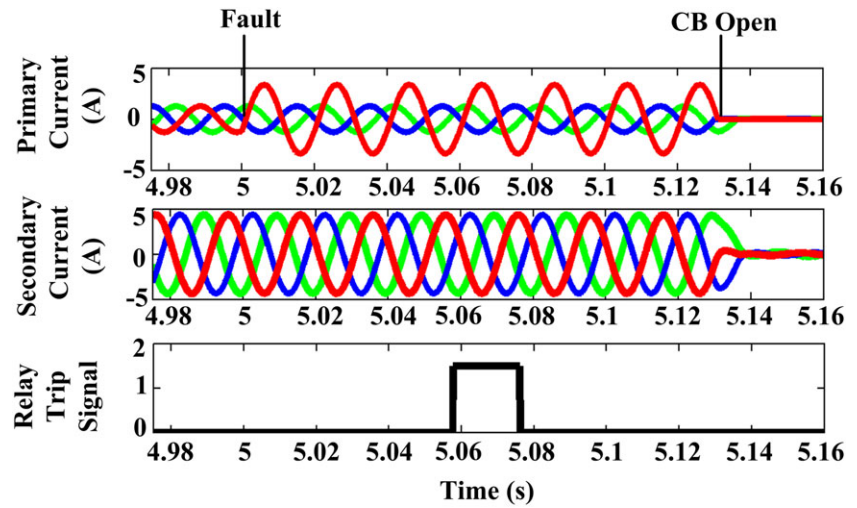


FIGURE 16 Primary current, secondary current, and trip signal of the differential relay when 10 wind generators are in service (internal fault)

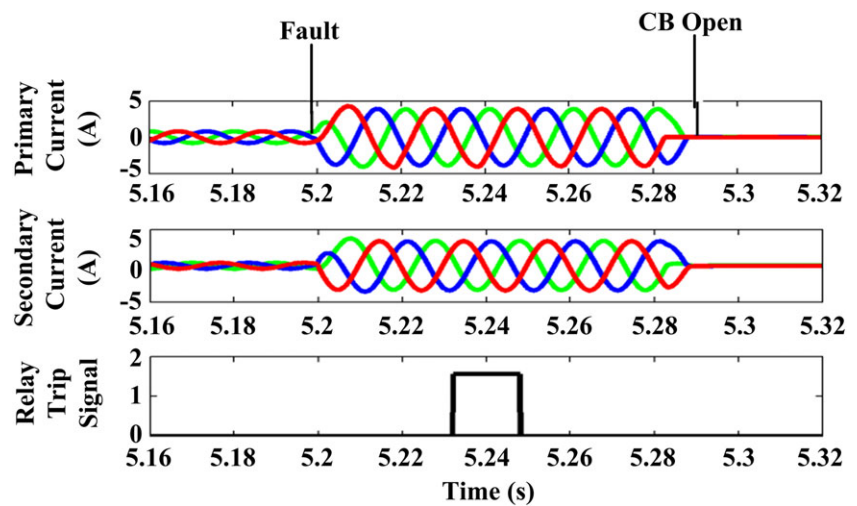


FIGURE 17 Primary current, secondary current, and trip signal of the differential relay when 10 wind generators are in service (external fault)

TABLE 5 Relay setting for dual slope differential relay (10 wind generators)

Wind Generators in Service	Pickup Current, A	K_1 (Initial Slope)	Crossover Point, A	K_m (Final Slope)
10	0.13	25	0.57	62

TABLE 6 Relay setting for dual slope differential relay (no wind generators in service)

Wind Generators in Service	Pickup Current, A	K_1 (Initial Slope)	Crossover Point, A	K_m (Final Slope)
Nil	0.13	25	0.57	70

The differential relay characteristics need to be modified with the new settings as shown in Table 5, in order to avoid mal-operation. The threshold value of the settings has to be changed by the removal of wind generators, due to the non-availability of wind.

The relay setting must be changed when there is no wind generator. When there is a fault in the feeders connecting wind farms to the grid or when there is no enough wind speed, the relay mal-operates. Table 6 presents the new relay settings which are required to avoid mal-functioning under this condition.

The differential relay settings are changed according to DG penetration. The percentage of SCIG penetration is determined by measuring the wind farm current. The differential relay setting is adaptively varied according to SCIG penetration. The threshold cannot be set as the exact values but must be varied accordingly with the wind power penetration level. The modified set of characteristics provides better sensitivity towards internal faults and more security to external faults.

5 | CONCLUSION

The sensitivity towards internal faults, as well as security with regard to external faults, of the transformer differential relay, can be improved by dual-slope characteristics. However, the conventional dual-slope characteristic needs to be modified in the presence of wind farms. The dual-slope differential protection for the substation transformer of a wind farm has been modeled, which discriminates internal faults from inrush, over excitation, and external fault conditions. The wind farm is simulated with a transformer differential protection scheme, while the differential relay mal-operates under external fault conditions as the wind power penetration changes. Mal-operation is avoided by introducing adaptiveness to differential relay characteristics. The differential relay parameter, ie, the final slope, is modified continuously according to changes in wind farm output in order to avoid mal-tripping. The modified algorithm is also validated using the experimental setup in the laboratory.

ACKNOWLEDGEMENT

The authors wish to thank the Department of Electrical Engineering of the National Institute of Technology Calicut and Kerala State Electricity Board (KSEB) Limited, Kerala, India for the support given to conduct this research.

LIST OF SYMBOLS

I_d	differential current
I_r	restraining current
I_1	transformer primary current
I_2	transformer secondary current
I_{pickup}	pickup current
K	lower percentage bias setting or initial slope
K_m	higher percentage bias setting or final slope
$I_{1intmin}$	minimum internal fault current at the primary side
$I_{2intmin}$	minimum internal fault current at the secondary side
$I_{1extmax}$	maximum external fault current at the primary side

$I_{2extmax}$	maximum external fault current at the secondary side
I_{rt}	bias current threshold setting or crossover point
I_{SC}	total short circuit current of the wind farm
I_w	short circuit current from a single wind generator
E''	sub transient internal voltage of the generator at the moment of short circuit
X''	sub transient reactance of the generator
V_t	terminal voltage of the generator
I_l	current of the wind generator
E_0	external fault operating point when none of the wind generators in the wind farm are in service
E_{100}	external fault operating point when all the wind generators in the wind farm are in service
I_{d1th}	threshold value of fundamental component of the differential current
I_{d2th}	threshold value of second harmonic component of the differential current
I_{d5th}	threshold value of fifth harmonic component of the differential current
I_{d1}	fundamental component of the differential current
I_{d2}	second harmonic component of the differential current
I_{d5}	fifth harmonic component of the differential current
I_{sim}	internal fault operating point during simulation
I_{exp}	internal fault operating point during experimentation
E_{2vsim}	simulated results for the external fault operating point, when 2 voltage sources at the secondary side of the transformer
E_{2vexp}	experimental results for the external fault operating point, when 2 voltage sources at the secondary side of the transformer
E_{1vsim}	simulated results for the external fault operating point, when 1 voltage source at the secondary side of the transformer
E_{1vexp}	experimental results for the external fault operating point, when 1 voltage source at the secondary side of the transformer
I_{WF}	total current from the wind farm
E_{19}	external fault operating point when 19 wind generators are in service
E_{10}	external fault operating point when 10 wind generators are in service

LIST OF ABBREVIATIONS

CT	current transformer
DG	distributed generation
PSCAD	power system computer-aided design
SCIG	squirrel cage induction generator

ORCID

Sujo Palamoottil George  <http://orcid.org/0000-0002-6375-1966>

Sankar Ashok  <http://orcid.org/0000-0002-1898-0903>

REFERENCES

1. Ellabban O, Abu-rub H, Blaabjerg F. Renewable energy resources: current status, future prospects and their enabling technology. *Renew Sustain Energy Rev.* 2014;39:748-764.
2. Ackermann T, Andersson G, Soder L. Distributed generation: a definition. *Electr Pow Syst Res.* 2001;57(3):195-204.
3. Nagamani C, Saravana Ilango G, Reddy MJB, Rani MAA, Lakaparampil ZV. Renewable power generation Indian scenario: a review. *Electr Power Components Syst.* 2015;43(8-10):1205-1213.

4. Alvarez-Herault MC, Picault D, Caire R, Raison B, HadjSaid N, Bienia W. A novel hybrid network architecture to increase DG insertion in electrical distribution systems. *IEEE Trans Power Syst.* 2011;26(2):905-914.
5. IEEE guide for protecting power transformers. *IEEE Standard C37.91-2008 (Revision of IEEE Std C37.91-2000).* 2008; 1-139.
6. Jenner R, Alencar N, Holanda U. A method to identify inrush currents in power transformers protection based on the differential current gradient. *Electr Pow Syst Res.* 2014;111:78-84.
7. Murugan SK, Simon SP, Sundareswaran K, Nayak PSR, Padhy NP. An empirical Fourier transform-based power transformer differential protection. *IEEE Trans Power Deliv.* 2017;32(1):209-218.
8. Oliveira LMR, Cardoso AJM. Application of Park's power components to the differential protection of three-phase transformers. *Electr Pow Syst Res.* 2012;83(1):203-211.
9. Fani B, Hamedani Golshan ME, Saghaian-nejad M. Transformer differential protection using geometrical structure analysis of waveforms. *Electr Power Components Syst.* 2011;39(3):204-224.
10. Rahmati A, Sanaye-Pasand M. A fast WT-based algorithm to distinguish between transformer internal faults and inrush currents. *Int Trans Electr Energy Syst.* 2011;22(4):471-490.
11. Sahebi A, Samet H. Identifying internal fault from magnetizing conditions in power transformer using the cascaded implementation of wavelet transform and empirical mode decomposition. *Int Trans Electr Energy Syst.* 2017;28(2):1-20.
12. Babnik T, Gubina F. Two approaches to power transformer fault classification based on protection signals. *Int J Electr Power Energy Syst.* 2002;24:459-468.
13. Samantaray SR, Dash PK. Decision tree based discrimination between inrush currents and internal faults in power transformer. *Int J Electr Power Energy Syst.* 2011;33(4):1043-1048.
14. Abniki H, Sanaye-pasand M. A novel technique for internal fault detection of power transformers based on moving windows. *Int Trans Electr Energy Syst.* 2013;24(9):1263-1278.
15. Ali E, Helal A, Desouki H, Shebl K, Abdelkader S, Malik OP. Power transformer differential protection using current and voltage ratios. *Electr Pow Syst Res.* 2018;154:140-150.
16. Hosny A, Sood VK. Transformer differential protection with phase angle difference based inrush restraint. *Electr Pow Syst Res.* 2014;115:57-64.
17. Zheng T, Shen H, Huang S, Chen P, Chen S. The effect of transformer non-synchronous energization on differential protection and its countermeasure. *Int Trans Electr Energy Syst.* 2015;26(2):309-322.
18. MiCOM P642, P643 and P645 transformer protection relay technical manual. *Schneider Electric.* 2010.
19. Transformer differential relays with percentage and harmonic restraint, types STD15C, STD16C relay manual. *GE Protection and Control.*
20. Sevov L, Khan U, Zhang Z. Enhancing power transformer differential protection to improve security and dependability. *IEEE Trans Ind Appl.* 2017;53(3):2642-2649.
21. Ballal MS, Umre BS, Suryawanshi HM. Sensitive incipient inter-turn fault detection algorithm for power transformers. *IET Electr Power Appl.* 2016;10(9):858-868.
22. Memon AA, Kauhaniemi K. A critical review of AC microgrid protection issues and available solutions. *Electr Pow Syst Res.* 2015;129:23-31.
23. Conti S. Analysis of distribution network protection issues in presence of dispersed generation. *Electr Pow Syst Res.* 2009;79(1):49-56.
24. Dingbian H, Duan J, Lei S, Yu H, Cui S. Applicability analysis of differential protection for dispersed wind generation in distribution network. *IEEE PES Asia-Pacific Power and Energy Conference* 2016:2148-2152.
25. Ojaghi M, Sudi Z, Azari M. Local online adaptive technique for optimal coordination of overcurrent relays within high voltage substations. *Int Trans Electr Energy Syst.* 2016;26(8):1810-1828.
26. Oliveira MO, Bretas AS, Ferreira GD. Adaptive differential protection of three-phase power transformers based on transient signal analysis. *Int J Electr Power Energy Syst.* 2014;57:366-374.
27. Dashti H, Sanaye-Pasand M. Power transformer protection using a multiregion adaptive differential relay. *IEEE Trans Power Deliv.* 2013;29(2):777-785.
28. Ashraf A, Mirsalim M, Masoum MAS. Application of a recursive phasor estimation method for adaptive fault component based differential protection of power transformers. *IEEE Trans Ind Informat.* 2017;13(3):1381-1392.
29. Operating manual for ASHIDA numerical transformer differential relay—type ADR 133A, ADR 233A. *ASHIDA Electronics Pvt. Ltd. India.* 2009.
30. Data sheet collected from the wind farms and wind integrated substation in Ramakkalmedu, owned and operated by Kerala State Electricity Board Limited, Kerala, India. *KSEB Ltd.* 2016

How to cite this article: George SP, Ashok S. Adaptive differential protection for transformers in grid-connected wind farms. *Int Trans Electr Energ Syst*. 2018;e2594. <https://doi.org/10.1002/etep.2594>

APPENDIX

TABLE A1 Transformer protection unit

Transformer	3 kVA, 415/415 V, Y-Y.
Differential protection	ASHIDA-ADR 133A, dual slope, harmonic restraint.
Over current + earth fault relay	L & T MC61A
Over voltage/under voltage relay	L & T MV12A
Power supply	3 phase, 415 V, 50 Hz

TABLE A2 Network details of the grid-connected wind farm

Wind turbine	Vestas-NM48 750 kW, cut-in speed-4 m/s, cut-out speed-25 m/s, rated speed-16 m/s
Generator	ELIN EBG MCM445L21F7Z 200/750 kW, 690 V D + D, 50 Hz, Rpm: 1006/1510 Full-load current (A): 200/705 Full-load torque (Nm): 1990/4890 Efficiency (%): 95.4/97 Power factor: 0.84/0.89 Mechanical input (kW): 210/773 Apparent power (kVA): 238/843 Reactive power (kVar): 130/385
Transformer	Transformers and Rectifiers India Ltd. 20 MVA, 66/33 KV,Y-Y
Differential relay	AREVA MiCOM P633 Dual slope, harmonic restraint
Current transformer	INSTRANS600/5 A, 1200/5 A
Grid	66 kV, fault level-1562 MVA